P3A.4   VALIDATION OF SNOW PARAMETERS AS DERIVED FROM DUAL-WAVELENGTH AIRBORNE RADAR

Liang Liao[1*], Robert Meneghini[2], Toshio Iguchi[3] and Andrew Detwiler[4]

[1]Caelum Research Corp., Code 975, NASA/GSFC, Greenbelt, MD 20771
[2]Code 975, NASA/GSFC, Greenbelt, MD 20771
[3]Communications Research Laboratory, Tokyo 184-8795, Japan
[4]South Dakota School of Mines & Technology, Rapid City, SD 57701

1.   INTRODUCTION

Dual-wavelength radar measurements can be used to estimate characteristics of the size distribution when one or both wavelengths operate in the non-Rayleigh region (Matrosov 1992; Meneghini et al 1992; Liao et al. 1997). A spaceborne radar operating at Ku and Ka bands has been proposed as one of the core instruments for the Global Precipitation Measurements (GPM) and will serve as a calibrator for other instruments aboard the GPM satellite in mapping precipitation globally. With use of dual-wavelength radar the ambiguities are significantly lessened for the retrieval of the microphysical properties of hydrometeors in comparison with single wavelength radars such as the TRMM PR. In this paper we begin with a discussion of a dual-wavelength algorithm by which the snow particle size distribution can be inferred. In an effort to examine its validity and accuracy, the algorithm is applied to measurements taken by a dual-wavelength (X and Ka bands) airborne radar during the Convective and Precipitation-Electrification Experiment (CaPE) in 1991. The retrieved results of the snow particle size distributions are then compared with those from in-situ aircraft measurements and the NCAR S- and X-band ground-based radars that were coordinated with the airborne radar measurements. Good agreement is found for these comparisons despite the uncertainties resulting from possible mismatches of the sample volumes among the different sensors as well as the spatial and temporal offsets.

2.   DUAL-WAVELENGTH ALGORITHM

The hydrometeor size distributions are well described by the Gamma function based on measurements and model studies. A form of the Gamma size distribution, N(D), used widely in the retrieval of the microphysical properties of hydrometeors, is expressed as

$$N(D) = N_0 D^\mu \exp\left[-(3.67+\mu)\frac{D}{D_0}\right]$$

where N_0 is constant, D the snow diameter, D_0 the median volume diameter of the snow particle and μ the shape factor. The number concentration, N_T, can be expressed in terms of these variables by:

$$N_T = N_0 \Gamma(\mu+1)/G^{\mu+1}$$

$$G = (3.67+\mu)/D_0$$

where Γ is the Gamma function. If μ is fixed the D_0 can be estimated from the measured values of the radar dual frequency ratio (DFR)

$$DFR = 10\log(Z_u/Z_v)$$

where Z_u and Z_v are the radar reflectivity factors at wavelengths of u and v. As an example, when u and v stand for the X band (10 GHz) and Ka band (35 GHz), respectively, Fig. 1 depicts the computational results of the DFR versus D_0 at several snow densities. The result shows that the DFR-D_0 relationship is nearly independent of the snow density if D_0 is less 3 mm. The computations of DFR at several values of μ (not shown) reveal that the DFR-D_0 relations are relatively insensitive to μ. In contrast, N_T is sensitive to the snow density and μ. For the snow region in stratiform storm where the attenuation is usually negligible for the airborne X and Ka band frequencies, D_0 can be directly estimated from the measured DFR. Note that the independence of the DFR on the snow density enables us to accurately estimate D_0. Once D_0 is known, N_T can be derived from the radar reflectivity at either wavelength once the snow density is either fixed or prescribed as a function of the snow particle size.
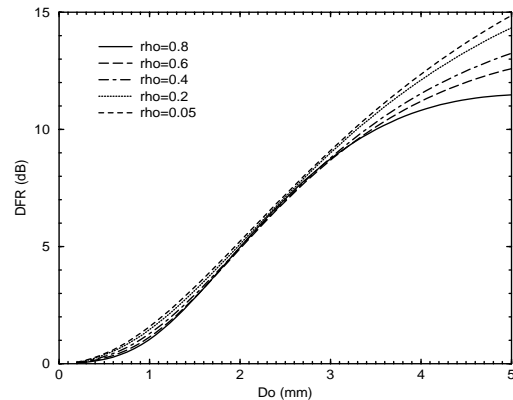

Fig.1   DFR at X and Ka bands versus snow D_0 for several snow densities for μ equal to 2.

* *Corresponding author address*: Liang Liao, Caelum Research Corp., Code 975, NASA/GSFC, Greenbelt, MD 20771; e-mail: lliao@priam.gsfc.nasa.gov.

To validate the estimates of D_0 and N_T, we focus in the following sections on the comparisons with in-situ airborne particle measurements as well as the drop size distribution parameters derived from S and X band ground-based radar.

3. COMPARISON WITH IN-SITU MEASUREMENTS

An airborne radar, built by the Communication Research Laboratory of Japan, was installed on the NASA T-39 aircraft. Operating at X- and Ka-bands, the radar viewed the precipitation at nadir with beamwidths matched at 5 degrees. The in-situ particle measurements were made using a PMS 2D-P probe mounted on the T-28 aircraft of the South Dakota School of Mines & Technology. On 19 July 1991 (UTC: 18:15-18:45) during the CaPE experiment, a weak convective cell was observed by airborne radar in coordination with in-situ measurements. Figure 2 illustrates the flight tracks of the T-39 and T-28 with an origin at longitude -81.2^o and latitude 28.35^o. The T-28 penetrated the storm twice where the start of track A occurred about 8 minutes before the start of the T-39 flight track leg and the start of track B about 3 minutes after the T-39 flight track. The offsets in space between the T-28 and T-39 were generally within 5 km. For these flights the T-39 flew at an altitude of approximately 11 km while the T-28 flew at 5.2 km. Figure 3a displays the T-39 measurements of the radar reflectivity at X band with respect to the flight track shown in Fig.2. The white line shown in Fig. 3a indicates the altitude of the T-28. The DFR derived from the X- and Ka-band data at 5.2 km is plotted in Fig.3b. Two regions can be clearly distinguished. Over the range from 3 to 7.5 km (region 1) the DFR attains levels as high as 6 dB whereas for distances exceeding 7.5 km (region 2) the average DFR is close to 1 dB. Regions 1 and 2 correspond to the T-39 time segments of 18:36:03-18:36:38 and 18:36:38-18:37:14, respectively, as shown in Fig.2. An examination of the T-28 PMS 2D-P images shows two main types of snow particles in this storm cell. For the period 18:28:45-18:29:47 for track A and 18:40:49-18:42:10 for track B, the particles appear to be almost exclusively aggregates. The particles viewed during the period 18:29:47-18:32:04 for track A and 18:39:20-18:40:49 for track B are identified as graupel from their small and nearly spherical shape. As such, we assume that the mass densities of these particles are between 0.4-0.8 g/cm^3. Since the attenuation is negligible in dry snow at these frequencies the D_0 is directly obtained from the DFR by use of the DFR-D_0 relations. Plotted in Fig.3c are the results of D_0 based on the DFR shown in Fig.3b. With use of D_0 and reflectivity at X band the N_T can be computed. The results are depicted in Fig.3d. To compare with the in-situ measurements, the T-28 data are projected onto the T-39 flight direction. To overcome possible offsets in space and time between the T-39 and T-28, an attempt is made to match the observations within the two regions by slightly shifting either starting or ending points of the T-28 flight tracks (shown in Fig.2) relative to the T-39. Thus the comparisons of the D_0 and
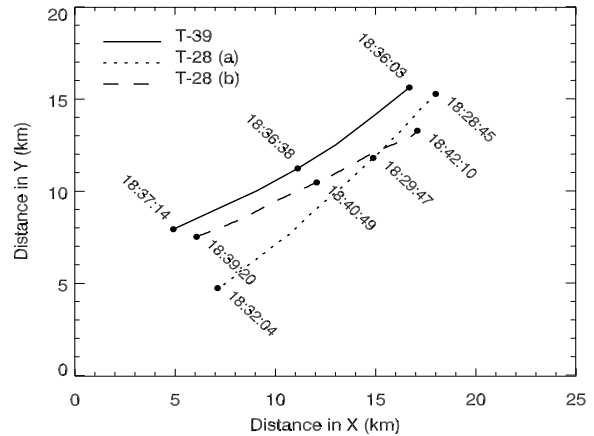

Fig.2 Flight tracks of the T-39 and T-28 aircraft during observations of a weak convective cell. Time stamps are given at selected positions.

N_T can be fairly made between the T-28 in-situ measurements and the T-39 airborne radar estimates. The results are illustrated in Fig.3c and 3d. In the estimation of D_0 and N_T from the T-39 radar, the particle densities of 0.1 g/cm^3 and 0.6 g/cm^3 are taken to characterize the aggregates and graupel in the two regions. The 2D-P measures the maximum dimension of the particle, either along the X or Y axis, whichever length is larger, so that the median volume diameter, $D_{0,max}$, is expressed in terms of the maximum dimension. Therefore, to compare the estimates of particle size from the in-situ and radar measurements an account must be made for the differences between $D_{0,max}$ and D_0. For the graupel particles which are nearly spherical, the $D_{0,max}$ and D_0 are approximately the same and therefore no adjustment is made. For the aggregates it is reasonable to assume that the $D_{0,max}$ is always larger than the D_0 which, by definition, is the equivalent-volume diameter of the sphere. To account for this difference, we have scaled the D_0 estimates from the dual-wavelength radar data by a factor of 1.5. Although the adjustment of D_0 to $D_{0,max}$ for aggregates depends on particle shape, orientation and size distribution, the scale factor of 1.5, used in Fig.3c, seems to work well for our comparisons. Note that the μ, the shape factor of the size distribution, is chosen as 2 for our retrievals, giving the best comparisons. As indicated in Fig.3, the retrievals of D_0 and N_T from the dual-wavelength radar measurements are fairly good. Some of the discrepancies between the retrieved and measured results may be attributable to offsets in the T-39 and T-28 flight tracks as well as the large differences between the sampling volumes of the radar and the PMS probe.

4. COMPARISON WITH GROUND-BASED RADAR

During CaPE the T-39 was also coordinated with measurements from the ground-based NCAR CP-2 radar that operated at S (3 GHz) and X bands. With the measurements of the CP-2 radar at two wavelengths

Fig.4 Map of the T-39 flight track (solid line) in reference to the NCAR CP-2 radar. The dashed line represents direction along which the RHI scan of the CP-2 was taken. Distances in km from the CP-2 are shown along the dashed line.
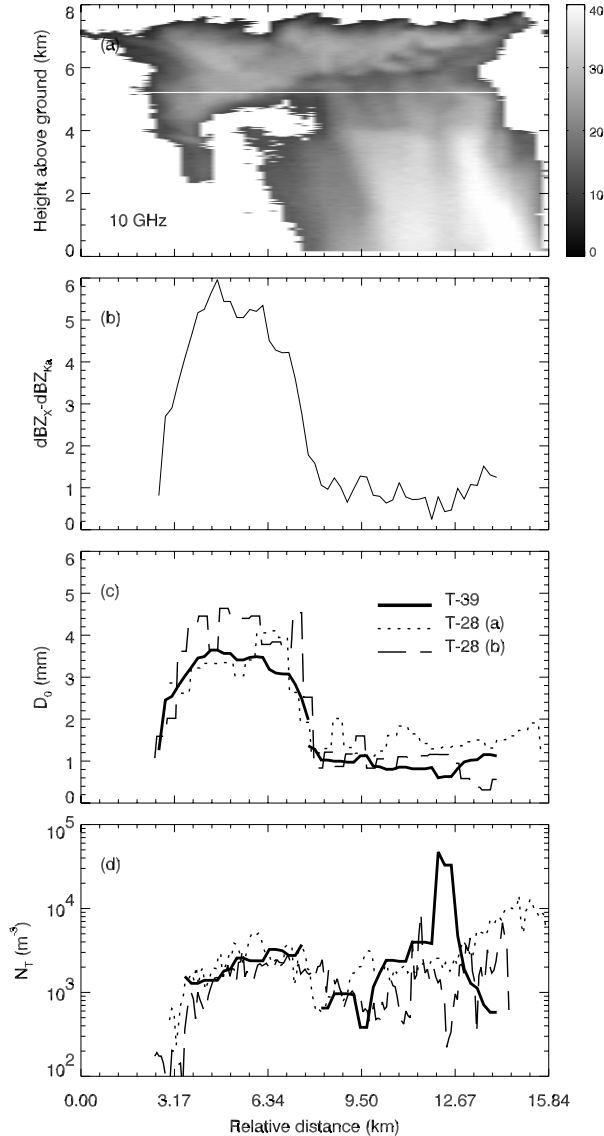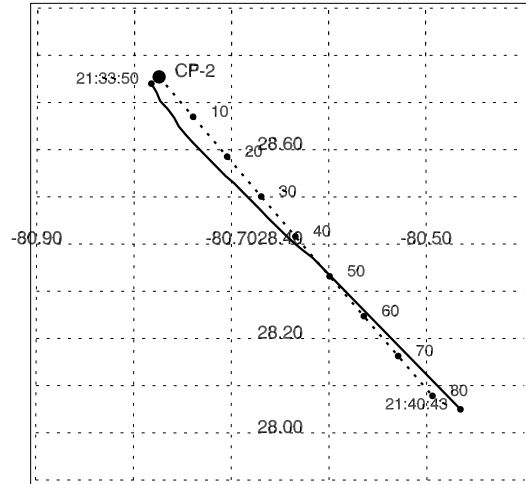
Fig.3 Airborne radar measurements over a weak convective cell and retrievals of the size distributions in comparisons with the in-situ particle measurements: (a) T-39 radar measured reflectivity at nadir along the flight track shown in Fig.2, (b) DFR of X and Ka bands at the altitude where the T-28 flew, as indicated by the white line in Fig.3a, (c) comparisons of D_0 between the radar estimated and the 2D-P measured results and (d) similar comparisons for N_T.

the D_0, in principle, can be estimated by the same procedure used for the X and Ka band data. As such, the consistency of the dual-wavelength radar algorithm can be further examined by comparing estimated parameters of the particle size distributions from the collocated measurements between the ground and airborne radars. Unlike the differences in the reflectivities between the X and Ka band data in snow, the values of DFR for S and X bands are relatively small and the measurements sometimes appear noisy. This

can be explained by the fact that the majority of the snow particles are much smaller than the S- and X-band wavelengths, and therefore their scattering is approximately characterized by the Rayleigh approximation in which the reflectivity is independent of the wavelength. Because of the small DFR the estimates of D_0 from the S and X bands require averaging over a sufficiently large number of measurements in time and space so that the DFR can be effectively extracted. In our analysis of the CP-2 radar the dual-wavelength algorithm is applied only to the mean profiles of DFR.

Shown in Fig.4 is one of the coordinated observations of the T-39 and CP-2 radars taken on 16 July 1991 over a stratiform portion of a storm. The T-39 flight track (solid line) is approximately collocated with the RHI scan (dashed line) of the CP-2 radar at 21:37:28. The measured reflectivities of the airborne and ground-based radars at X band are displayed in Fig.5 with respect to the distances from the CP-2 radar. Both radars exhibit very similar structures of the storm despite a gap (missing data) in the T-39 radar data. With its fairly high vertical resolution (30 m) the bright band is well defined by the T-39 airborne radar. For the case of the CP-2 radar where the vertical resolution degrades gradually as the horizontal range increases, the bright band is clearly detected only for distances less than about 40 km. To compare the T-39 and CP-2 radar estimates, the data are used only if the reflectivities measured from both radars exceed their minimum detectable signals. Plotted in Fig.6 are their vertical (top) and horizontal (bottom) profiles of the D_0 estimated from the mean profiles of DFR in the snow region (above radar bright band). As can be seen from the figure, the D_0 from the CP-2 exhibits large fluctuations but nevertheless shows a clear trend in the both vertical and horizontal directions. These trends are
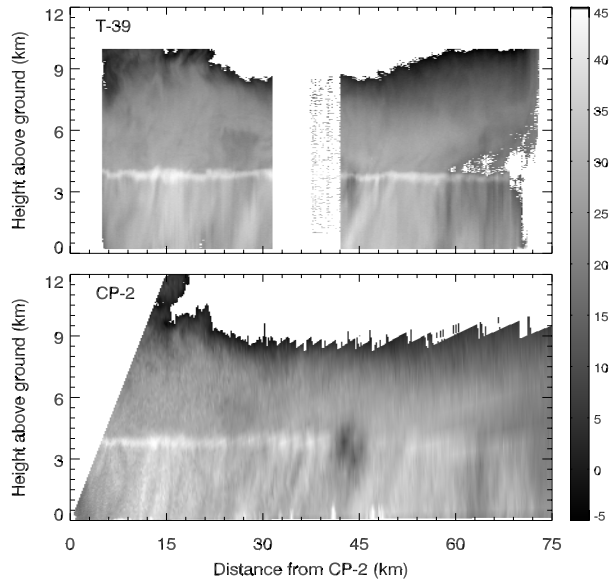
Fig.5 Radar measured reflectivities of the T-39 airborne radar (top) and the CP-2 ground radar (bottom). The data, collocated in terms of the distance from the CP-2, are taken at X band, corresponding to the T-39 flight track and the scan direction (dash line) shown in Fig.4 for the airborne and ground-based radars.

generally consistent with those from the T-39 radar which provide much more stable results. Overall, the estimates of D_0 of the T-39 and CP-2 radars are correlated fairly well for both the vertical and horizontal profiles. It should be mentioned here that the profiles of D_0 in Fig.6 are derived at a snow density of 0.2 g/cm^3 with μ set to 2. However, as noted earlier, the results do not change significantly if other values of either snow density or μ are used. It should also be noted that the results of N_T from the CP-2 radar (not shown) fluctuate strongly because of the dependence on the snow density and D_0. As a result of this uncertainty, the comparisons of N_T are not instructive.

5. SUMMARY

A description was presented of a dual wavelength radar algorithm to estimate characteristics of the snow size distribution. The fact that the DFR depends primarily on D_0 suggests that accurate estimates of the particle size distributions should be possible if the particles are sufficiently large relative to the shorter wavelength and if the attenuation can be either neglected or corrected. Having carefully registered the particle information obtained from the aircraft in-situ PMS measurements on the airborne radar, the radar-derived characteristic parameters of the size distributions are compared with the measurements. We find that the radar results agree reasonably well with those from the direct measurements by the PMS. Also compared are the estimates of D_0 between the
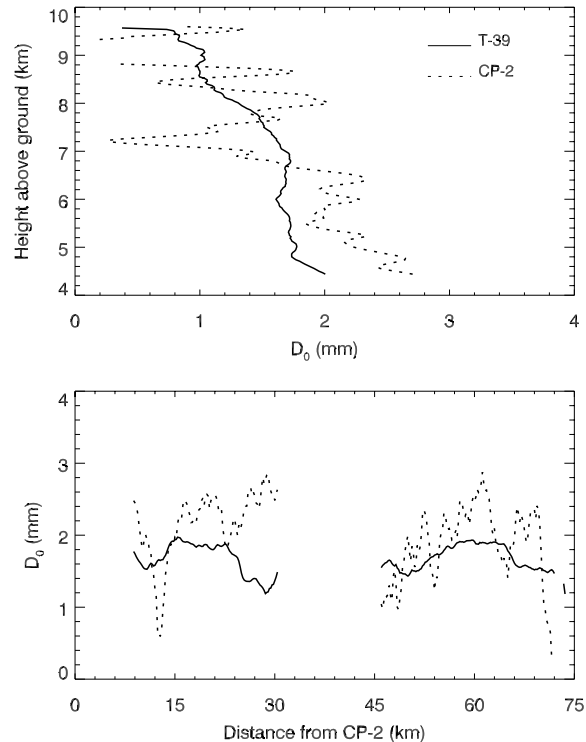

Fig.6 Comparisons of the vertical (top) and horizontal (bottom) profiles of D_0 as derived from the T-39 airborne and CP-2 ground-based radars in the snow region.

dual-wavelength airborne and ground-based radars from one of their coordinated measurements, showing that the retrievals of D_0 from both radars are to some extent consistent. We conclude that the use of dual-wavelength radar, with properly chosen wavelengths, may provide reliable estimates of the microphysical properties of hydrometeors.

6. ACKNOWLEDGEMENTS

We wish to thank NCAR for providing the CP-2 radar data and its processing software. T-28 operations were supported by the NSF Lower Atmospheric Observing Facilities program

7. REFERENCES

Liao, L., R. Meneghini, T. Iguchi and A. Detwiler, 1997: Estimation of snow parameters from dual-wavelength airborne radar. Preprints 28th Conf. Radar Meteor., American Meteor. Soc., 510-511.

Matrosov, S. Y., 1992: Radar reflectivity in snowfall. *IEEE Trans. Geosci. Remote Sens.*, **30**, 454-461.

Meneghini, R., T. Kozu, H. Kumagai, and W. C. Boncyk, 1992: A study of rain estimation methods from space using dual-wavelength radar measurements at near-nadir incidence over ocean. *J. Atmos. Oceanic Technol.*, **9**, 364-382.